J Math Chem (2013) 51:1521–1531
DOI 10.1007/s10910-013-0161-8

ORIGINAL PAPER

Solving for the time-dependent multi-configuration hartree fock equations based on sine-discrete variable representation

Wenliang Li

Received: 13 September 2012 / Accepted: 11 March 2013 / Published online: 21 March 2013

Abstract A parallel quantum electrons wave packet computer code has been developed to study laser-atom interaction in the nonperturbative regime with attosecond resolution. The motion equations of the multi-configuration time-dependent hartree fock (MCTDHF) based on a sine discrete variable representation were solved by using an adaptive stepsize Runge-Kutta integrator of eight orders. Some efficient algorithms and strategies to accelerate the calculation velocity are introduced and discussed in details. Some illustrated imaginary time propagation and real time propagation have been respectively done in the paper. Single ionization probabilities calculated by using this one dimension MCTDHF model underestimate the accurate results calculated by solving time-dependent Schrodinger equation directly.

Keywords Laser-atom interaction · Sine discrete variable representation · Finite basis representation · MCTDHF

1 Introduction

In recent years, there has been increasing interest in the correlated dynamics of many-electron systems. Theorists have developed a variety of explicit time-dependent versions of electronic structure methods [1–15]. Most of the explicitly time-dependent approaches to quantum chemistry yet, were mainly carried out on the density functional (TD-DFT) [1,2], the Hartree–Fock (TD-HF) level of theory [3,4], or the configuration interaction (TD-CI) method [5]. An important method known as multi-configuration

W. Li (✉)
State key Laboratory of Molecular Reaction Dynamics, Dalian Institute of Chemical Physics, Chinese Academy of Science, Dalian 116023, China
e-mail: wenliangli.dicp@gmail.com

W. Li
Xinjiang Institute of Engineering, Urumqi, Xinjiang 830091, China

time-dependent Hartree Fock (MCTDHF) has been developed in the last few years [6–15]. It can either be seen as an explicitly time-dependent version of the complete active space self-consistent field method, or a specialization of the well established multi-configuration time-dependent Hartree (MCTDH) method [16–19] for distinguishable nuclei. A unified and compact form of MCTDH has been developed to specify for systems of identical particle (MCTDHF for fermions MCTDHB for bosons) [20–22]. Alon et al. [23] have derived a multiconfigurational time-dependent Hartree theory for systems with particle conversion. The theory thus extends the scope of the available and successful multiconfigurational time-dependent Hartree methods-which were solely formulated for and applied to systems with a fixed number of particles-to a broader class of physical systems and problems. Followed the accurate multi-boson long-time dynamics in triple-well periodic traps were studied [24]. Later MCTDHF was applied to study the two-photo ionization of helium by Hochstuhl et al. [25]. Just recently, we have demonstrated the use of MCTDHF method to compute double ionization of helium [26]. A new version of single layer MCTDHF theory in second quantization representation based on a decomposition of the overall Fock space has been also introduced by the author [27].

A large part of computation time is spent with the evaluation of the time-dependent mean field matrix and other time-dependent one/two-electron spin orbital integrals in MCTDHF frame [8,12]. The accuracy and efficient calculation of mean field matrix is the crucial step to study the electron-electron correlated dynamics of systems interacting with laser field. The calculation of mean field matrix is related to the calculation of the two-electron integrals in DVR or sine FBR. So the details study of the methods to accelerate the calculation velocity of the two-electron integrals and mean field matrix are necessary and important. The efficient algorithms to accelerate the calculation velocity have been investigated in this paper.

2 Theory

In this section, some crucial aspects of MCTDHF are introduced. We follow the standard notation of the multi-configuration time-dependent Hartree (MCTDH) method for nuclear quantum dynamics [16–19] and those presented by Nest et al. [11–15]. Atomic units have been used throughout the paper, unless stated otherwise.

In MCTDHF, the N-electron wave function can be linearly combined into time-dependent Slater determinants.

$$\begin{aligned}\Psi(\vec{x_1},\vec{x_2},....\vec{x_N},t) &= \frac{1}{\sqrt{N!}}\sum_J A_J(t)|\chi_{j_1}(\vec{x_1},t)...\chi_{j_N}(\vec{x_N},t)| \\ &= \frac{1}{\sqrt{N!}}\sum_J A_J(t)|\ J,t\rangle. \end{aligned} \tag{1}$$

The coefficient tensors A_J as well as the spin-orbitals $\chi_{j_1}(\vec{x_1},t)$ are time-dependent. The capital letter J is a composite index which enumerates the number of spin-orbitals N_{spin} appearing in the determinant, and $\vec{x_i} = (\vec{r_i}, s_i)$ is a composite variable for the position $\vec{r_i}$ and the spin coordinate s_i.

The Hamiltonian describing the N-electron system, which interacts with the strong laser field, can be expressed as follows:

$$H = \sum_{i=1}^{N} \frac{p_i^2}{2} + \sum_{i=1}^{N} (V(r_i)) + \sum_{i}^{N} \sum_{i>j}^{N} \frac{1}{r_{ij}}. \tag{2}$$

The external potential $V(r_i)$ is produced by the (fixed) nuclei $V_{nuc}(r_i)$ and may also contains the coupling to an additional laser field in the dipole approximation $V_{external}(r_i)$. Then the variational principle is used for the coefficients and spin orbitals, respectively,

$$\left\langle \delta\Psi(t) \left| H - i\frac{\partial}{\partial t} \right| \Psi(t) \right\rangle = 0. \tag{3}$$

The corresponding equations of motion A_J and $\chi_{j_1}(\vec{x_1}, t)$ are obtained

$$i\frac{dA_J}{dt} = \frac{1}{N!} \sum_{L} \langle J|H|L\rangle A_L, \tag{4}$$

$$i\frac{d\chi}{dt} = (1-P)\rho^{-1} \langle H\rangle \chi. \tag{5}$$

where $P = \sum_i \mid \chi_i \rangle \langle \chi_i \mid$ is the projector operator on the space spanned by the single particle functions, $\rho_{ij} = \left\langle \frac{\partial\Psi}{\partial\chi_i} \middle| \frac{\partial\Psi}{\partial\chi_j} \right\rangle$ is the density operator, $\langle H\rangle_{ij} = \left\langle \frac{\partial\Psi}{\partial\chi_i} \middle| H \middle| \frac{\partial\Psi}{\partial\chi_j} \right\rangle$ is the so-called mean field operator.

In the derivation of the working equation, we choose the Sine-DVR grid function ξ_k. That is, the space orbital φ_i is combined with grid function, $\varphi_i = \sum_k C_{i,k}\xi_k$, and the spin orbital is expressed as follows,

$$\chi_i = \varphi_i * s_i = s_i * \sum_k C_{i,k}\xi_k. \tag{6}$$

We then rewrite Eq. (4) into an algebraic expression,

$$i \begin{pmatrix} \frac{dA_1}{dt} \\ \frac{dA_2}{dt} \\ \frac{dA_3}{dt} \\ \cdots \end{pmatrix} = \frac{1}{N!} \begin{pmatrix} \langle J_1|H|J_1\rangle & \langle J_1|H|J_2\rangle & \langle J_1|H|J_3\rangle & \cdots \\ \langle J_2|H|J_1\rangle & \langle J_2|H|J_2\rangle & \langle J_2|H|J_2\rangle & \cdots \\ \langle J_2|H|J_1\rangle & \langle J_2|H|J_2\rangle & \langle J_2|H|J_2\rangle & \cdots \\ \cdots & \cdots & \cdots & \cdots \end{pmatrix} \begin{pmatrix} A_1 \\ A_2 \\ A_3 \\ \cdots \end{pmatrix}. \tag{7}$$

Each matrix element in the algebraic equation can be solved by the Slater rules [28].

The key to obtain the algebraic form of Eq. (5) depends on the derivation of matrix element of the mean field operator $\langle H\rangle_{ij} = \left\langle \frac{\partial\Psi}{\partial\chi_i} \middle| H \middle| \frac{\partial\Psi}{\partial\chi_j} \right\rangle$, here $\left| \frac{\partial\Psi}{\partial\chi_j} \right\rangle$ is a single-hole function. On the basis of the nuclear dynamics method, we assume that electron 1

is missing. After derivation and reformulation, we find that the single-hole function $|\ \frac{\partial\Psi}{\partial\chi_j}\rangle$ is also a combination of Slater determinants, in which the coordinate of electron 1 is absent.

$$\left|\ \frac{\partial\Psi}{\partial\chi_j}\right\rangle = \sum_M A_M|\ M\rangle\,. \tag{8}$$

It is important to emphasize that there are only $N_{spin}-1$ spin orbitals in the Slater $|\ M\rangle$ because the coordinates of the missing electron 1 are absent.

According to Eq. (8) and the expression of the element of the mean field operator $\left\langle\frac{\partial\Psi}{\partial\chi_i}\ \middle|H|\ \frac{\partial\Psi}{\partial\chi_j}\right\rangle$, we obtain,

$$\left\langle\frac{\partial\Psi}{\partial\chi_i}\ \middle|H|\ \frac{\partial\Psi}{\partial\chi_j}\right\rangle = \sum_M\sum_L A_M A_N\,\langle M\ |H|\ L\rangle. \tag{9}$$

Then we can decompose the Hamiltonian of this system into four parts,

$$H(r_1,r_2,r_3,...) = h(r_1) + \sum_1\sum_{i>1}\frac{1}{r_{1i}} + \sum_{i>1}h(r_i) + \sum_{i>1}\sum_{j>i}\frac{1}{r_{ij}}. \tag{10}$$

The first term is the single electron Hamiltonian term of electron 1, the second one is the coulomb interaction between electron 1 and all other electrons. The last two parts do not contain the coordinates of electron 1, and will not contribute to the calculation after a projection of $P = \sum_i |\ \chi_i\rangle\,\langle\chi_i\ |$, in which only contains the coordinates of electron 1.

Combined Eq. (9) with Eq. (10), we get the elements of the mean field operator,

$$\begin{aligned}
&\sum_M\sum_L A^*_{i,M}A_{j,N}\,\langle M|H|L\rangle\\
&= \sum_M\sum_L A^*_{i,M}A_{j,N}\left\langle M\middle|h(r_1) + \sum_1\sum_{i>1}\frac{1}{r_{1i}}\middle|L\right\rangle\\
&= \sum_M\sum_L A^*_{i,M}A_{j,N}\,\langle M|h(r_1)|L\rangle + (f-1)*\sum_M\sum_L A^*_{i,M}A_{j,N}\left\langle M\middle|\frac{1}{r_{12}}\middle|L\right\rangle\\
&= h(r_1)\rho_{i,j} + (f-1)*\sum_M\sum_L A^*_{i,M}A_{j,N}\left\langle M\middle|\frac{1}{r_{12}}\middle|L\right\rangle.
\end{aligned} \tag{11}$$

The first part in the atomic basis functions can be expressed as,

$$\rho_{i,j}\,\langle\xi\ |h(r_1)|\ \zeta\rangle\,. \tag{12}$$

where $|\ \zeta\rangle$ and $|\ \xi\rangle$ are grid basis functions.

For the second part of Eq. (11), only the spin orbital with coordinate 2 is involved since the Slater determinants $|\ L\rangle$ and $|\ M\rangle$ do not contain the coordinates of electron 1,

$$\sum_{j_2}\sum_{k_2}\sum_{j_3}\cdots\sum_{j_f} A^*_{i,j_2,j_3..j_f} A_{j,k_2,j_3..j_f} \left\langle \chi_{j_2} \left| \frac{1}{r_{12}} \right| \chi_{k_2} \right\rangle. \tag{13}$$

Inserting Eq. (6) into Eq. (14), we obtain

$$\sum_{j_2}\sum_{k_2}\sum_{j_3}\cdots\sum_{j_f} A^*_{i,j_2,j_3..j_f} A_{j,k_2,j_3..j_f} \left\langle \left(\sum_k C_{j_2,k}\xi_k\right)^* \left| \frac{1}{r_{12}} \right| \left(\sum_k C_{k_2,k}\xi_k\right) \right\rangle \delta_{s_i s_j}. \tag{14}$$

In the above expression, $\delta_{s_i s_j}$ is a Delta function. We can easily get the matrix element in grid basis functions,

$$\begin{aligned} &\left\langle \zeta_p \right| \sum_{j_2}\sum_{k_2}\sum_{j_3}\cdots\sum_{j_f} A^*_{i,j_2,j_3..j_f} A_{j,k_2,j_3..j_f} \left\langle \left(\sum_k C^*_{j_2,k}\xi_k\right) \left| \frac{1}{r_{12}} \right| \left(\sum_l C_{k_2,l}\xi_l\right) \right\rangle \left| \xi_u \right\rangle \delta_{s_i,s_j} \\ &= \sum_{j_2}\sum_{k_2}\sum_{j_3}\cdots\sum_{j_f} A^*_{i,j_2,j_3..j_f} A_{j,k_2,j_3..j_f} \sum_{k\in\xi}\sum_{l\in\xi} C^*_{j_2,k} C_{k_2,l} \left\langle \xi_k \zeta_p \left| \frac{1}{r_{12}} \right| \xi_l \xi_u \right\rangle \delta_{s_i,s_j}. \end{aligned} \tag{15}$$

The element $\left\langle \xi_k \zeta_p \left| \frac{1}{r_{12}} \right| \xi_l \xi_u \right\rangle$ in Eq. (15) is the two-electron integral in the grid basis function space. The details calculation method was followed.

3 Algorithms

3.1 Sine-DVR

The sine-DVR was chosen in the calculation which was commonly used in theoretical studies of nuclear reaction dynamics [16–19]. The sine DVR uses the particle-in-a-box eigen-functions as a basis. The box boundaries are x_0 and x_{N+1}, and $L = x_{N+1} - x_0$ denotes the length of the box. The basis functions are thus

$$\left\{ \varphi_j(x) = \sqrt{2/L}\sin(j\pi(x - x0)/L),\ j = 1, 2, ...N \right\} \text{ for } x_0 \le x \le x_{N+1} \tag{16}$$

The corresponding grid points basis functions are $\{X_i(x), i = 1, 2, ...N\}$, and the corresponding grid value are $\{x_i, i = 1, 2, ...N\}$.

3.2 Mode of atom

For the simplicity, we take one dimension (1D) helium system for example. The total time-dependent Hamiltonian for 1D helium atom irradiated by a laser fields $\varepsilon(t)$ reads

$$\begin{aligned} H(x, y, t) = &-\frac{1}{2}\frac{d^2}{dx^2} - \frac{1}{2}\frac{d^2}{dy^2} - \frac{2}{\sqrt{x^2 + b^2}} - \frac{2}{\sqrt{y^2 + b^2}} + \frac{1}{\sqrt{(x - y)^2 + b^2}} \\ &+(x + y)\varepsilon(t) \end{aligned}$$

where the electron-electron interaction and the electron-nucleus interaction are modeled by the usual 'smoothed Coulomb' potential with shielding parameter b. In order to solve MCTDHF equations, the two-electron integrals in grid basis functions in DVR or sine basis function in finite basis representation (FBR) must be calculated. The two-electron integrals in grid basis functions in DVR read,

$$TWO_{DVR} = \iint\limits_{x\ y} X_\alpha^*(x) X_\beta(x) \frac{1}{\sqrt{((x-y)^2+b^2)}} X_\sigma^*(x) X_\delta(x) dxdy \tag{17}$$

Those calculations of integrals will consume much time and memory [6,8]. Up to now, a significant approximation can be obtained with the expansion,

$$\widetilde{V_{ee}}(x, y) = \sum_{m=1}^{M} U_m(x) * V_m(y) \tag{18}$$

with changing a two-dimensional integrations into $2M$ one-dimension integrations. In the paper, we have tried to do an accurate integration calculation in the sine-FBR.

$$TWO_{FBR} = \iint\limits_{x\ y} \varphi_i^*(x) \varphi_j(x) \frac{1}{\sqrt{((x-y)^2+b^2)}} \varphi_k^*(x) \varphi_l(x) dxdy \tag{19}$$

which was solved by using Gaussian quadrature method with six orders.

The method can be used to be staff gauge to identify the accuracy of the above approximation method. The two-folds integration Gaussian quadratrue formula with weigths ω_i and nodes x_i reads (nd is the number of nodes)

$$\int_{-1}^{1}\int_{-1}^{1} f(x, y) dxdy = \sum_{i=1}^{nd}\sum_{j=1}^{nd} \omega_i \omega_j f(x_i, y_i) \tag{20}$$

3.3 Optimization strategy

The matrix elements of $\langle J_i \,|H|\, J_j \rangle$ in slater determine basis in Eq. 7 need to be calculated during at every propagation step. The matrix elements of $\langle J_i \,|H|\, J_j \rangle$ are of conjugate symmetry. Only lower triangle parts of elements are calculated in the soft package. The elements are stored in a linear array. For the simplicity, we take a 4*4 matrix for example. As can be seen from Fig. 1, the ten elements of lower triangle need to be calculated in the processing. The arrow sequence is the order of the address stored in the linear array. In order to search the corresponding memory address quickly when row and column are given, an index array Ia is necessary. $Ia(i) = i * (i-1)/2, i = 1, ..N$, in where N is the matrix dimension. The address of term (i_row, i_column) is $Ia(\max(i\_row, i\_column)) + \min(i\_row, i\_column)$. It is obvious that the corresponding address of a_{32}, a_{43} is respectively $5 = Ia(3) + 2$ and $9 = Ia(4) + 3$.

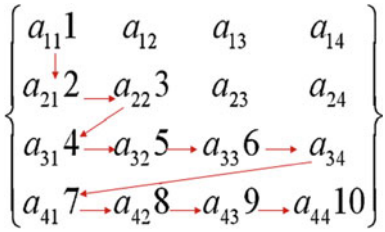

Fig. 1 An example symmetry or conjugate symmetry matrix with 4*4. Only the *lower triangle* ten elements are remembered and calculated

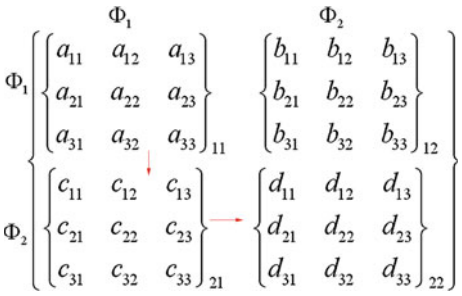

Fig. 2 An example of mean field matrix expression, with two number of spins orbitals and three number of grid basis function

In order to calculate the matrix elements $\langle J_i|H|J_j\rangle$ in Eq. 7, time-dependent one-electron spin orbital integral ($\langle\chi_i|h_1|\chi_i\rangle$) and two-electron spin orbital integrals ($[\chi_i\chi_j|\chi_k\chi_l] = \int \chi_i^*(x)\chi_j(x)V_{ee}\chi_k^*(y)\chi_l(y)dxdy$) need to be calculated at every step during propagation. When all the elements of $\langle J_i\ |H|\ J_j\rangle$ are calculating, many two-electron spin orbital integrals are repeatedly calculated. In order to accelerate the velocity of calculation, all two-electron spin orbitals integrals are classified by using itself symmetry before MCTDHF calculation. When the propagate time update, only the unique two-electrons spin orbitals integrals are calculated for the following MCTDHF propagation.

The expression of mean field operator is defined in Eqs. 9 and 11. It is a complicated embed matrix, whose detailed matrix expression can be found in Fig. 2 (assume there are two spin orbitals and three grid basis functions). The mean field matrix is of complex-conjugate symmetry $\left[H_{\alpha\beta}\right]_{ij} = \left[H_{\alpha\beta}\right]_{ji}^*$. It is obvious that $\left[b_{\alpha\beta}\right]_{ij} = \left[c_{\alpha\beta}\right]_{ji}^*$ in Fig. 2. In the calculation, there are N_{spin} spin orbitals. There are total $N_{spin}*(N_{spin}+1)/2$ elements which are evenly calculated by N_{procs} processors. By taking advantage of the properties of the grid basis functions in DVR, Eq. 17 can be simplified by

$$TWO_{DVR} = \sum_{m=1}^{M} \delta_{\alpha,\beta}U_m(x_\alpha)\delta_{\sigma,\delta}V_m(x_\sigma) \tag{21}$$

It is clearly that not every two-electron integrals need to be calculated; only parts of those which are not-zero are necessary. By combining with Eqs. 15, 21 and the properties of grid basis functions, only the diagonal element of mean field elements $\left[H_{\alpha\beta}\right]_{ij} = \delta_{\alpha\beta}\left[H_{\alpha\alpha}\right]_{ij}$ is non-zeros.

4 Illustrated calculations and discussions

4.1 Test of the efficiency of the source code

In order to test the efficiency of the algorithms used in our source code, helium atom was calculated with grid range from -30 to 30 $a.u.$ by using various number of grid points. The calculated results are listed in Table 1. It can be seen that with the increase of the number of the grids and the number of the spatial orbital used in the calculation, the advantage and the efficient of algorithm used in our source code is more obvious. The MPI source code for solving MCTDHF working equations is available upon request.

4.2 Imaginary time propagation

To test the accuracy and the stability of our Fortran source code, we take typical two-electron system, the helium atom, for example. Firstly we obtain the ground state energy of helium atom through the propagation in imaginary time (PIT) in the absence of an external laser field. We firstly consider the influence of the number of the active space on the atom relaxation energy when the wave function propagates in imaginary time. The calculated results are shown in Fig. 3. We increase the active space from 1 spatial orbitals and 1 determinant [CAS(1,2), HF)], to 8 spatial orbitals and 120 determinant CAS(8,2). When the number of active space increases, the relaxed energy becomes lower. The relaxed energy of the PIT of CAS(8,2) is 2.899 hartree which is nearly equal to the full configuration energy (about 2.90 hartree) of helium atom. When a guess state which is a hybrid state was initialized, it will relax to the ground state during the processing of imaginary propagation. With the elapse of the imaginary time, more and more excited states were erased. The accurate ground state electron density distribution obtained by using the imaginary propagation with CAS(8,2) is plotted in Fig. 4 when the propagation finished.

Table 1 Total propagation time is 20 a.u. . nr is the number of grid points

	Serial version without optimization	Serial version with optimization	Serial version with optimization +MPI [nprocs = 2]	Serial version with optimization +MPI [nprocs = 8]
[−30, 30]nr = 100 CAS(2,2)	61 mins	4 mins	2 mins	
[−30, 30]nr = 200 CAS(2,2)	533 mins	28 mins	15 mins	
[−30, 30]nr = 100 CAS(4,2)	750 mins	20 mins	12 mins	3 mins
[−30, 30]nr = 200 CAS(4,2)	7,000 mins	128 mins	68 mins	19 mins

Grid range is from [−30, 30]. Active space is respectively CAS(n,2), n is the number of the spatial orbital. The number of electrons is 2

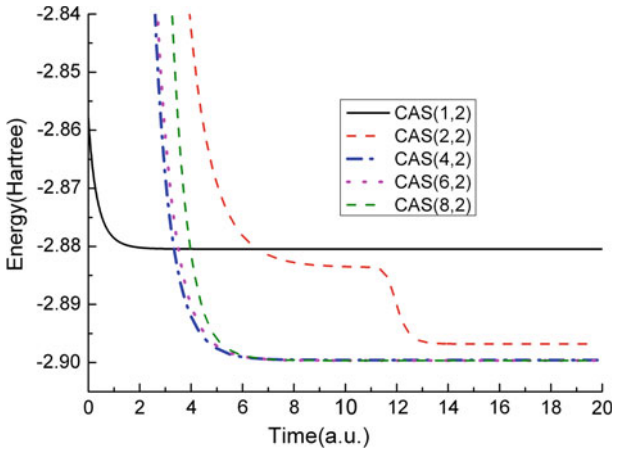

Fig. 3 The influence of the active space on the imaginary time process and the last ground state energy

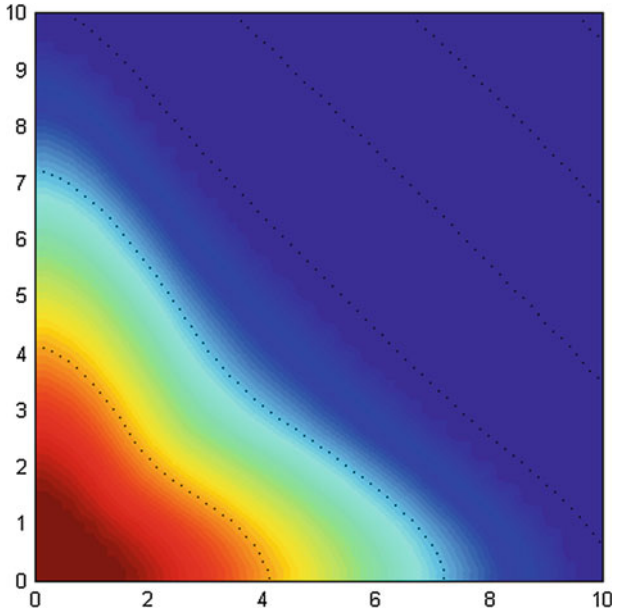

Fig. 4 The end ground state got by using imaginary time propagation

4.3 Real time propagation

After the accurate ground state wave functions are obtained by using PIT, we can then further investigate the interaction between laser pulse and helium atom. In the calculation, we choose 20(24) spin orbitals for the two active electrons system to produce 190(276) singlet determinants. The gird points range are from -100 to 100 with the number of grid points = 500. In order to proof our calculation, the same laser

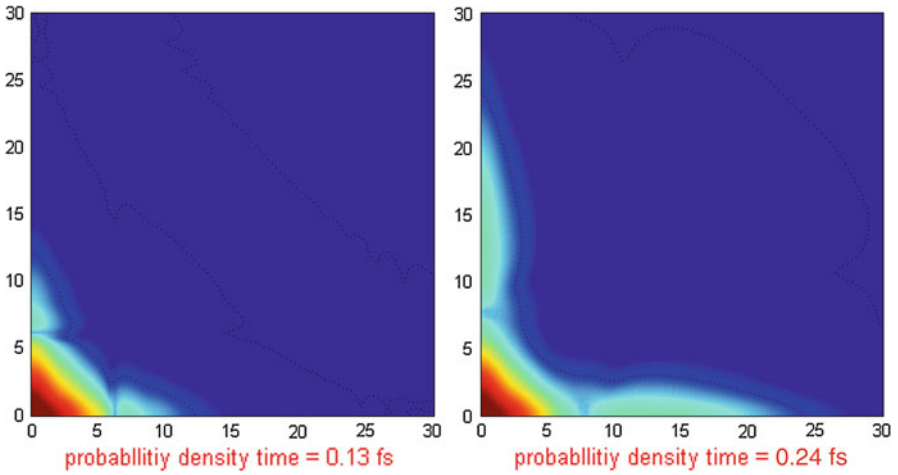

Fig. 5 The wave function probability distribution in different time during real time propagation processing

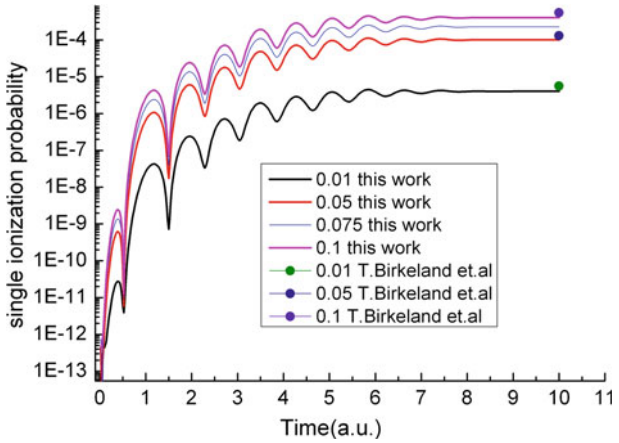

Fig. 6 Single ionization probability of helium atom during four different intensity laser field

field was selected as in the recently reports about accurate theoretical calculations of helium atom in strong laser field which were attained by solving time dependent Schrodinger equation [29]. The left panel of Fig. 5 is the electrons probability distribution at time=0.13 fs. It is obvious that electrons are moving far away in the force of laser field. The right panel of Fig. 5 is the electrons probability distribution at time = 0.24 fs. It can be found that parts of electrons probability distribution are far away from the core nuclei. It is obvious that single ionization take place during the propagation. The single ionization probabilities are calculated in four difference intensity laser field. The calculated results are illustrated in Fig. 6. The black line, red line, blue line and pink line are respectively the results for laser intensity $\varepsilon = 0.01, 0.05, 0.075, 0.1$a.u. The green point, navy point and violent point are the results in reference [29] for laser intensity $\varepsilon = 0.01, 0.05, 0.1$a.u. The continuously increasing population peaks

indicates the electron wave packets scatter mostly away from the core nuclei. When the direction of the laser field reverse, the dropping population peaks occur due to the returning wave packets driven by the laser field recombines to the core nuclei. It is obvious that our results agree well with the accurate ones. Our results are slightly below their results due to the simple model used in our calculation.

5 Conclusion

The motion equations of MCTDHF were solved by using an adaptive stepsize runge-kutta integrator of eight orders and based on a sine discrete variable representation (Sin-DVR). Some efficient algorithms to solve the motions equations of MCTDHF are introduced and discussed. Real time propagation results indicate that the single ionization probabilities calculated with simple model underestimate the accurate results obtained by solving time-dependent Schrodinger equation directly.

References

1. E. Runge, E.K.U. Gross, Phys. Rev. Lett. **52**, 997 (1984)
2. F. Calvayrac, P.G. Reinhard, E. Suraud, C.A. Ullrich, Phys. Rep. **337**, 493 (2000)
3. K.C. Kulander, Phys. Rev. A **36**, 2726 (1987)
4. M.S. Pindzola, P. Gavras, T.W. Gorczyca, Phys. Rev. A **51**, 3999 (1995)
5. T. Klamroth, Phys. Rev. B **68**, 245421 (2003)
6. J. Zanghellini, M. Kitzler, C. Fabian, T. Brabec, A. Scrinzi, Laser Phys. **13**, 1064 (2003)
7. J. Zanghellini, M. Kitzler, T. Brabec, A. Scrnzi, J. Phys. B At. Mol. Opt. Phys. **37**, 763 (2004)
8. J. Caillat, J. Zhanghellini, M. Kitzler, O. Koch, W. Kreuzer, A. Scrinzi, Phys. Rev. A **71**, 012712 (2005)
9. T. Kato, H. Kono, Chem. Phys. Lett. **392**, 533 (2004)
10. T. Kato, Kaoru Yamanouchi, J. Chem. Phys. **131**, 164118 (2009)
11. M. Nest, T. Klamroth, P. Saalfrank, J. Chem. Phys. **122**, 124102 (2005)
12. M. Nest, T. Klamroth, Phys. Rev. A **72**, 012710 (2005)
13. M. Nest, J. Theor. Comput. Chem. **6**, 563 (2007)
14. M. Nest, Phys. Rev. A **73**, 023613 (2006)
15. M. Nest, R. Padmanaban, P. Saalfrank, J. Chem. Phys. **126**, 214106 (2007)
16. H.D. Meyer, U. Manthe, L.S. Cederbaum, Chem. Phys. Lett. **165**, 73 (1990)
17. M.H. Beck, A. Jackle, G.A. Worth, H.D. Meyer, Phys. Rep. **324**, 1 (2000)
18. M. Nest, H.D. Meyer, J. Chem. Phys. **119**, 24 (2003)
19. H.D. Meyer, U. Manthe, L.S. Cederbaum, J. Chem. Phys. **97**, 3199 (1992)
20. O.E. Alon, A.I. Streltsov, L.S. Cederbaum, Phy. Rev. A **76**, 062501 (2007)
21. O.E. Alon, A.I. Streltsov, L.S. Cederbaum, J. Chem. Phys. **127**, 154103 (2007)
22. O.E. Alon, A.I. Streltsov, L.S. Cederbaum, Phy. Rev. A **77**, 033613 (2008)
23. O.E. Alon, A.I. Streltsov, L.S. Cederbaum, Phys. Rev. A **79**, 022503 (2009)
24. A.I. Streltsov, K. Sakmann, O.E. Alon, L.S. Cederbaum, Phys. Rev. A **83**, 043604 (2011)
25. D. Hochstuhl, M. Bonitz, J. Chem. Phys. **134**, 084106 (2011)
26. W.L. Li, W.W. Xu, Mol. Phys. **111**, 119 (2013)
27. W.L. Li, W.W. Xu, K.L. Han, J. Theor. Comput. Chem. **12**, 1250105 (2013)
28. A. Szabo, N.S. Ostlund, Modern quantum chemistry, introduction to advanced electronic structure theory, Mineola, New York. 1996, 1–466
29. T. Birkeland, R. Nepstad, M. Førre, Phys. Rev. Lett. **104**, 163002 (2010)